RESEARCH ARTICLE

Human Mutation

OFFICIAL JOURNAL
HGVS
HUMAN GENOME VARIATION SOCIETY
www.hgvs.org

A Loss-of-Function Variant in the Human Histidyl-tRNA Synthetase (*HARS*) Gene is Neurotoxic In Vivo

Aimée Vester,[1] Gisselle Velez-Ruiz,[2] Heather M. McLaughlin,[1] NISC Comparative Sequencing Program,[3] James R. Lupski,[4–6] Kevin Talbot,[7] Jeffery M. Vance,[8] Stephan Züchner,[8] Ricardo H. Roda,[9] Kenneth H. Fischbeck,[9] Leslie G. Biesecker,[10] Garth Nicholson,[11,12] Asim A. Beg,[2]* and Anthony Antonellis[1,13]*

[1]*Department of Human Genetics, University of Michigan Medical School, Ann Arbor, Michigan;* [2]*Department of Pharmacology, University of Michigan Medical School, Ann Arbor, Michigan;* [3]*NIH Intramural Sequencing Center, National Human Genome Research Institute, National Institutes of Health, Bethesda, Maryland;* [4]*Department of Molecular and Human Genetics, Baylor College of Medicine, Houston, Texas;* [5]*Department of Pediatrics Baylor College of Medicine, Houston, Texas;* [6]*Genetics, Texas Children's Hospital,, Houston, Texas;* [7]*Department of Clinical Neurology, University of Oxford, Oxford, United Kingdom;* [8]*Hussman Institute for Human Genomics, University of Miami Miller School of Medicine, Miami, Florida;* [9]*Neurogenetics Branch, National Institute of Neurological Disorders and Stroke, National Institutes of Health, Bethesda, Maryland;* [10]*Genetic Disease Research Branch, National Human Genome Research Institute, National Institutes of Health, Bethesda, Maryland;* [11]*Northcott Neuroscience Laboratory, ANZAC Research Institute and Molecular Medicine Laboratory, Concord Hospital, Concord, New South Wales, Australia;* [12]*Faculty of Medicine, University of Sydney, Camperdown, New South Wales, Australia;* [13]*Departments of Neurology, University of Michigan Medical School, Ann Arbor, Michigan*

Communicated by Ming Qi

Received 21 April 2012; accepted revised manuscript 24 August 2012.
Published online 28 August 2012 in Wiley Online Library (www.wiley.com/humanmutation). DOI: 10.1002/humu.22210

ABSTRACT: Aminoacyl-tRNA synthetases (ARSs) are ubiquitously expressed enzymes responsible for ligating amino acids to cognate tRNA molecules. Mutations in four genes encoding an ARS have been implicated in inherited peripheral neuropathy with an axonal pathology, suggesting that all ARS genes are relevant candidates for disease in patients with related phenotypes. Here, we present results from a mutation screen of the histidyl-tRNA synthetase (*HARS*) gene in a large cohort of patients with peripheral neuropathy. These efforts revealed a rare missense variant (c.410G>A/p.Arg137Gln) that resides at a highly conserved amino acid, represents a loss-of-function allele when evaluated in yeast complementation assays, and is toxic to neurons when expressed in a worm model. In addition to the patient with peripheral neuropathy, p.Arg137Gln *HARS* was detected in three individuals by genome-wide exome sequencing. These findings suggest that *HARS* is the fifth ARS locus associated with axonal peripheral neuropathy. Implications for identifying ARS alleles in human populations and assessing them for a role in neurodegenerative phenotypes are discussed.
Hum Mutat 34:191–199, 2013. © 2012 Wiley Periodicals, Inc.

KEY WORDS: aminoacyl-tRNA synthetases; peripheral neuropathy; *HARS*; neurotoxicity

Introduction

Peripheral neuropathies are a heterogeneous class of disorders mainly characterized by distal motor and sensory dysfunction. Etiological classifications for peripheral neuropathies include acquired, syndromic, and inherited neuropathy, each of which can be further subdivided into axonal or demyelinating forms [Dyck and Lambert, 1968]. The prevalence of peripheral neuropathy can exceed 10% in aging populations, making this class of diseases a major public healthcare concern in terms of proper diagnosis, prognosis, and therapeutic development [Martyn and Hughes, 1997]. The prevalence and heterogeneity of peripheral neuropathies underscore the importance of identifying genetic lesions that directly cause or modify clinical phenotypes.

Aminoacyl-tRNA synthetases (ARSs) are ubiquitously expressed, essential enzymes that perform the first step of protein translation—attaching amino acids to cognate tRNA molecules [Antonellis and Green, 2008]. Despite the ubiquitous function of ARSs, mutations in four loci encoding an ARS enzyme have been implicated in dominant and recessive peripheral neuropathies with an axonal pathology: glycyl-tRNA synthetase (*GARS*; MIM# 600287), tyrosyl-tRNA synthetase (*YARS*; MIM# 603623), alanyl-tRNA synthetase (*AARS*; MIM# 601065), and lysyl-tRNA synthetase (*KARS*; MIM# 601421) [Antonellis et al., 2003; Jordanova et al., 2006; Latour et al., 2010; McLaughlin et al., 2010]. These data indicate that genes encoding ARS enzymes are relevant candidates for disease in patients with peripheral neuropathy and no known contributing genetic variation.

The full complement of ARS loci and alleles implicated in peripheral neuropathy remains undefined. Addressing this issue will aid in determining if peripheral nerve axons are susceptible to mutations in a specific subset of ARS enzymes or if mutations in any ARS enzyme will result in a peripheral neuropathy. Furthermore, the mechanistic link between ARS mutations and neurodegeneration has not been identified and many disease-associated alleles have not been evaluated for neurotoxicity in vivo. Establishing an approach for rapidly characterizing alleles in the 37 human ARS-encoding genes will be critical for advancing our understanding of ARS-related

*Correspondence to: Anthony Antonellis, University of Michigan Medical School, 3710A Medical Sciences II, 1241 E. Catherine St. SPC 5618, Ann Arbor, MI 48109. E-mail: antonell@umich.edu or Asim A. Beg, University of Michigan Medical School, 1301D MSRB III, 1150 W. Medical Center Dr., Ann Arbor, MI 48109. E-mail: asimbeg@umich.edu

Contract Grant Sponsor: National Institute of Neurological Diseases and Stroke (grants NS060983 to A.A., R01NS052767 to S.Z., and U54NS065712 to S.Z.); Intramural Research Programs of the National Human Genome Research Institute and National Institute of Neurological Diseases and Stroke (National Institutes of Health).

neurodegeneration. Here, we present data from patient-based mutation screening, yeast complementation assays, and a worm model of neurotoxicity that reveal a loss-of-function, neurotoxic histidyl-tRNA synthetase (*HARS*) variant. Our findings raise the possibility that *HARS* mutations are associated with axonal peripheral neuropathy and further support a role for impaired tRNA charging in the pathogenesis of ARS-related peripheral neuropathy.

Materials and Methods

HARS Mutation Analysis

DNA samples were isolated from 363 patients diagnosed with peripheral neuropathy by collaborating physicians. DNA samples from the ClinSeq™ cohort were collected as previously described [Biesecker et al., 2009]. The appropriate review boards of each participating institution approved these studies. The *HARS* gene was assessed for mutations at the NIH Intramural Sequencing Center (NISC) as previously described [McLaughlin et al., 2010]. Each *HARS* variant was independently confirmed via PCR amplification followed by DNA sequencing analysis. Nucleotide positions are relative to the open reading frame from GenBank Accession No. NM_002109.3. Nucleotide numbering reflects cDNA position with +1 corresponding to the A of the ATG translation initiation codon in the reference sequence. Codon numbering for the HARS protein was based on the reported amino acid sequence (NCBI accession no. NP_002100.2). The initiation codon is codon 1. The variants were submitted to an LSDB at www.LOVD.nl/HARS.

Control Sample Genotyping

A total of 576 DNA samples isolated from neurologically normal controls were obtained from the National Institute of Neurological Diseases and Stroke (NINDS) and Coriell Institute for Medical Research (Panel numbers NDPT079, NDPT082, NDPT084, NDPT090, NDPT093, and NDPT094) and genotyped for each *HARS* variant using MassARRAY® iPLEX Gold technology (Sequenom, San Diego, CA). Briefly, multiplex *HARS*-specific PCR reactions were performed (primer sequences available upon request) followed by primer extension assays using mass-modified dideoxynucleotide terminators. MALDI-TOF mass spectrometry was used to determine the genotype for each individual using SpectroTYPER software (Sequenom). The presence of each *HARS* variant in the general population was additionally assessed using the Exome Variant Server (snp.gs.washington.edu/EVS/), the 1000genomes database (www.1000genomes.org/), and dbSNP (www.ncbi.nlm.nih.gov/snp).

Multispecies Comparative Sequence Analysis

HARS protein orthologs from multiple species were derived from the following GenBank accession numbers: Human (*Homo sapiens,* NP_002100.2), Mouse (*Mus musculus,* NP_032240.3), Chicken (*Gallus gallus,* NP_001006144.1), Zebrafish (*Danio rerio,* NP_001004586.1), Nematode (*Caenorhabditis elegans,* NP_001023373.1), Fruit Fly (*Drosophila melanogaster,* NP_728180.1), Baker's Yeast (*Saccharomyces cerevisiae*, AAA34696.1), and Bacteria (*Escherichia coli,* NP_289067.1). Amino acid sequences were aligned using Clustal W2 (http://www.ebi.ac.uk/Tools/clustalw2/index.html).

Computational Predictions of Pathogenicity

Each HARS protein variant was analyzed using the MUPro (http://www.ics.uci.edu/~baldig/mutation.html), PolyPhen (http://genetics.bwh.harvard.edu/pph/index.html), PolyPhen2 (http://genetics.bwh.harvard.edu/pph2/), and SIFT (http://sift.jcvi.org/www/SIFT_seq_submit2.html) prediction algorithms.

Yeast Complementation Assays

DNA constructs for yeast complementation assays were generated using Gateway cloning technology (Invitrogen, Carlsbad, CA). The *S. cerevisiae HTS1* locus (including the open reading frame and 477 base pairs of proximal promoter sequence) were PCR amplified using *S. cerevisiae* genomic DNA. Each primer was designed to include flanking Gateway attB1 (forward) and attB2 (reverse) sequences (primers available upon request). Subsequently, purified PCR products were recombined into the pDONR221 vector (according to the manufacturer's instructions) to yield an appropriate entry clone; the insert of the final entry clone was sequenced to confirm specificity. Mutagenesis of *HTS1* was performed using the QuikChange II XL Site-Directed Mutagenesis Kit (Stratagene, Santa Clara, CA) and appropriate mutation-bearing oligonucleotides. Subsequently, plasmid DNA purified from each entry clone was recombined with a gateway-compatible pRS315 or pRS316 destination vector according to the manufacturer's instructions. Each resulting expression construct was analyzed by restriction enzyme digestion with *Bsr*GI (New England Biosystems, Ipswich, MA) to confirm the presence of an appropriately sized insert.

A commercially available diploid heterozygous *hts1*Δ yeast strain (MATa/α, *his3*Δ1/*his3*Δ1, *leu2*Δ0/*leu2*Δ0, *LYS2*/*lys2*Δ0, *met15*Δ0/*MET15*, *ura3*Δ0/*ura3*Δ0; Open Biosystems, Hunstville, AL) was transformed with a *URA3*-bearing pRS316 vector containing wild-type *HTS1* (see above). Lithium acetate transformations were performed at 30°C using 200 ng of plasmid DNA, as previously described [Green et al., 1999]. Transformation reactions were grown on yeast medium lacking uracil. Subsequently, sporulation and tetrad dissections were performed to obtain a haploid *hts1*Δ strain that also contains the wild-type *HTS1* pRS316 maintenance vector. Briefly, the transformed diploid *hts1*Δ strain was patched twice onto presporulation plates (5% D-glucose [Fisher Scientific, Hampton, NH], 3% nutrient broth [Becton, Dickinson and Company, Franklin Lakes, NJ], 1% yeast extract [Acros Organics, Waltham, MA], and 2% agar [Teknova, Hollister, CA]). One microliter of cells was then transferred into 2 ml of supplemented liquid sporulation medium (1% potassium acetate [Fisher Scientific], 0.005% zinc acetate [Fisher Scientific], 1X ura supplement [MP Biomedicals, Solon, OH], 1X his supplement [MP Biomedicals], and 1X leu supplement [MP Biomedicals]) and incubated for 5 days at 25°C followed by 3 days at 30°C. Sporulated strains were dissected using a MSM 400 dissection microscope (Singer Instruments, Somerset, UK), and plated on yeast extract, peptone, and dextrose (YPD) plates (Becton, Dickinson and Company). Resulting spores were individually patched onto solid growth medium containing Geneticin (G418) or 0.1% 5-fluoroorotic acid (5-FOA), or media lacking uracil (Teknova). Two spores that grew on G418 and yeast medium lacking uracil, yet did not grow on 5-FOA medium, were selected for use in the yeast viability assays. Two resulting haploid *hts1*Δ strains bearing a wild-type *HTS1* pRS316 maintenance vector were then transformed with *LEU2*-harboring pRS315 constructs containing wild-type or mutant *HTS1* (described above) and grown on medium lacking uracil and leucine (Teknova). For each transformation, five colonies were selected for additional analysis.

Each colony was diluted in 100 μl H_2O, then further diluted 1:10 and 1:100, and spotted on growth medium containing 0.1% 5-FOA (Teknova), incubated for 3 days at 30°C, and growth was assessed by visual inspection. Because 5-FOA is toxic to yeast cells bearing a functional *URA3* allele, only cells that lost the *URA3*-bearing maintenance plasmid and for which the *LEU2*-harboring test plasmid could complement the chromosomal *hts1*Δ allele were expected to grow. To generate growth curves, surviving yeast colonies from strains modeling p.Val238Ala and p.Pro505Ser *HTS1* were inoculated in selective medium and incubated shaking overnight at 30°C. Dilutions were generated in YPD medium to obtain an OD_{660} of 0.05, and cultures incubated shaking at 30°C. The OD_{660} was then measured at 1, 2, 3, 4, 5, 6, 7, and 25 hours using a NanoDrop 1000 (Thermo Fisher Scientific, Waltham, MA). The percent increase in growth was determined by dividing each of the measured OD_{660} values by the initial OD_{660} value and expressing relative to the wild-type *HTS1*-harboring strain.

C. elegans Strains and Genetics

Standard methods for maintaining *C. elegans* were used [Brenner, 1974]. Bristol strain N2 was used as the wild type, and all animals were grown at 20°C. All *C. elegans* strains were obtained from the *C. elegans* Genetics Stock Center, University of Minnesota, Minneapolis.

C. elegans Transgene Construction

C. elegans transgene constructs were made from the expression vector pPD157.60 (Addgene, Firelab vector kit), which contains promoter sequences from the *C. elegans* glutamic acid decarboxylase (*unc-25*) gene. Expression of *C. elegans* wild-type or mutant *hars-1* cDNAs were engineered by cloning sequence verified full-length wild type or mutant R137Q cDNA sequences into the *Xba*I/*Nae*I sites of pPD157.60. Green fluorescent protein (GFP) fusion constructs were engineered using a PCR fusion approach to generate in-frame *N*-terminal tagged P*unc-25*::GFP-*hars-1* (WT or R137Q) plasmids [Hobert, 2002].

Transgenic *C. elegans* Strain Construction

Transgenic *C. elegans* strains were generated by standard microinjection techniques [Mello et al., 1991]. All transgenic strains were injected with plasmids of interest at 50 ng/ml + 2.5 ng/ml pCFJ90 (P*myo-2*::mCherry) + 47.5 ng/ml 1 Kb+ DNA Ladder (Invitrogen). For all strains, stable transgenic lines were selected based on mCherry expression in the pharyngeal muscles from a P*myo-2*:mcherry coinjection marker. At least three independent lines were isolated and analyzed. The data shown are from one representative line.

Phenotypic Scoring in *C. elegans*

Movement defects were quantified by counting the number of body thrashes in liquid for a 2-min interval [Miller et al., 1996]. Specifically, 100 μl of room temperature M9 media was aliquoted into an agar-coated 96 well plate. Individual animals were picked to wells and allowed to acclimate for 2 min. Movement was recorded using a cooled monochrome camera (Leica) and the number of times animals bent across their body axis was counted. To allow for accurate scoring of body bends, the image sequence was played at one-quarter speed offline using ImageJ. The total number of body bends counted was divided by two, yielding a body thrash/minute count.

Quantification of Neuronal Defects in *C. elegans*

Motor neuron quantification was performed on the following strains: EG1285: *oxIs12* (Punc-47::GFP; lin-15b) X, BEG9: *oxIs12* (Punc-47::GFP, lin-15b) X; aabEx8 (Punc-25::hars-1 [WT], Pmyo-3::mCherry), BEG10 : *oxIs12* (Punc-47::GFP, lin-15b) X; aabEx9 (Punc-25::hars-1 [R137Q], Pmyo-3::mCherry), BEG11: aabEx10 (Punc-25::GFP-hars-1 [WT], Pmyo-3::mCherry), BEG12: aabEx11 (Punc-25::GFP-hars-1 [R137Q], Pmyo-3::mCherry). Synchronized fourth larval stage worms were grown at 20°C. L4, 1-day, and 4-day adults were selected for imaging and phenotypic characterization. To visualize axonal processes, transgenic worms were anesthetized in M9 buffer containing 5 mM levamisole, mounted on agar pads and then coverslipped. To quantify the percent animals exhibiting aberrant GABA motor neurons commissures, >100 animals/genotype/timepoint were imaged. Animals exhibiting at least one aberrant commissure were scored as positive.

Microscopy

Animals were imaged on a Leica DMI6000B compound microscope with a CCD camera (FDC360, Leica) using a 40X objective. Confocal images were obtained on a Nikon A1R microscope with a 20X objective.

Results

Mutation Analysis of the *HARS* Locus

We screened the *HARS* gene for protein-coding variations in 363 patients with peripheral neuropathy and no previously identified mutation (the appropriate, institute-specific review boards approved all studies performed herein, and informed consent was obtained from all subjects). These efforts revealed six *HARS* missense variants in the heterozygous state in eight patients from our cohort: c.14C>A which predicts p.Ala5Glu, c.410G>A which predicts p.Arg137Gln, c.605G>A which predicts p.Gly205Asp, c.713T>C which predicts p.Val238Ala, c.1127A>G which predicts p.Lys376Arg, and c.1513C>T which predicts p.Pro505Ser (Table 1).

To determine the frequency of each identified *HARS* variant we tested for the presence of each in five available resources: (1) dbSNP (locus identifier 3035); (2) the NINDS/Coriell neurologically normal control panels (NDPT079, NDPT082, NDPT084, NDPT090, NDPT093, and NDPT094); (3) the Exome Variant Server (EVS; snp.gs.washington.edu/EVS/); (4) the 1000genomes database (browser.1000genomes.org); and (5) the ClinSeq™ patient cohort [Biesecker et al., 2009]. This revealed the presence of p.Ala5Glu, p.Arg137Gln, p.Gly205Asp, and p.Lys376Arg *HARS* in one or more of these analyses, whereas p.Val238Ala and p.Pro505Ser *HARS* were not detected in any of the five resources (Table 1). We also collected DNA samples from additional affected and unaffected family members related to the two carriers of p.Gly205Asp *HARS* and the single carrier of p.Lys376Arg *HARS*. Neither of these variants segregate with disease status in the three pedigrees (data not shown). Additional family members were not available to test for segregation of the remaining four variants with disease status.

To predict the pathogenic potential of the identified *HARS* variants we assessed the evolutionary conservation of each affected

Table 1. Identification of *HARS* Variants in Patients with Peripheral Neuropathy

cDNA change[a]	Amino acid change[b]	Patient chromosomes	NINDS control chromosomes	EVS chromosomes	1000genomes chromosomes	ClinSeq™ chromosomes	dbSNP accession no.
c.14C>A	p.Ala5Glu	2/726	10/1,066	86/10,670	8/2,188	9/1,130	rs78741041
c.410G>A	p.Arg137Gln	1/726	0/1,088	1/10,757	1/2,188	1/1,148	rs191391414
c.605G>A	p.Gly205Asp	2/726	3/1,022	15/10,743	7/2,188	2/1,146	rs147288996
c.713T>C	p.Val238Ala	1/726	0/1,092	NP	NP	NP	NP
c.1127A>G	p.Lys376Arg	1/726	0/1,090	62/10,696	3/2,188	NP	rs139447495
c.1513C>T	p.Pro505Ser	1/726	0/1,088	NP	NP	NP	NP

[a]Nucleotide positions are relative to the open reading frame from GenBank Accession number NM_002109.3.
[b]Amino acid positions are relative to GenBank Accession number NP_002100.2.
NP, not present.

Table 2. Computational Predictions of *HARS* Variant Pathogenicity

Variant	MUPro[a]	PolyPhen[b]	PolyPhen2[c]	SIFT[d]
p.Ala5Glu	0.20	0.34	0.00	1.00
p.Arg137Gln	−1.00[e]	2.46[e]	1.00[e]	0.00[e]
p.Gly205Asp	0.00	0.71	0.28	0.00[e]
p.Val238Ala	−1.00[e]	1.90[e]	0.78	0.00[e]
p.Lys376Arg	0.48	1.41	0.01	0.31
p.Pro505Ser	−.99[e]	2.01[e]	0.31	0.00[e]

[a]MUPro scores <0 indicate a decrease in protein stability.
[b]PolyPhen scores ≥1.5 indicate a prediction of "pathogenic."
[c]PolyPhen2 scores ∼1 indicate a prediction of "pathogenic."
[d]SIFT scores ≤0.05 indicate a prediction of "pathogenic."
[e]Denotes a "pathogenic" prediction.

Table 3. Human HARS Variants Modeled in the Yeast Ortholog HTS1

Human HARS[a]	Yeast HTS1[b]
p.Arg137Gln	p.Arg116Gln
p.Gly205Asp	p.Lys184Asp
p.Val238Ala	p.Val217Ala
p.Lys376Arg	p.Lys371Arg
p.Pro505Ser	p.Val519Ser

[a]Amino acid coordinates correspond to GenBank accession number NP_002100.2.
[b]Amino acid coordinates correspond to GenBank accession number AAA34696.1.

amino acid. Briefly, we collected the protein sequences of HARS orthologs from multiple, evolutionarily diverse species, aligned the sequences with ClustalW2 software [Larkin et al., 2007], and visually inspected each affected amino acid (Fig. 1B). Alanine 5 resides in a region of the protein sequence that is difficult to align, and is conserved among three of the five species analyzed. Arginine 137 is conserved among all species analyzed, including bacteria—indeed, this amino acid residue is invariant among all available protein sequences [Freist et al., 1999]. Glycine 205 is conserved among six of the eight species analyzed, including worm and fruit fly. Valine 238 is conserved among seven of the eight species analyzed, including yeast. Lysine 376 is conserved among four of the eight species analyzed, all of which are vertebrate species. Finally, proline 505 also resides in a region of the protein sequence that is difficult to align and is conserved among two of the eight species analyzed.

We applied computational predictions to further assess the potential effect of each *HARS* variant on protein function using the MuPro, PolyPhen, PolyPhen2, and SIFT algorithms [Cheng et al., 2006] (Table 2), which have been employed to assess disease-associated ARS mutations [McLaughlin et al., 2010]. The *HARS* variants p.Ala5Glu and p.Lys376Arg were not predicted to be pathogenic by any of the algorithms, and p.Gly205Asp was only predicted to be pathogenic by one of the four algorithms. In contrast, p.Val238Ala and p.Pro505Ser were predicted to be pathogenic by three of the four algorithms, and p.Arg137Gln was predicted to be pathogenic by all four algorithms employed.

We next mapped each variant onto the primary structure of the HARS protein (Fig. 1C). Alanine 5 is located at the first amino acid of the WHEP-TRS domain, which is predicted to mediate the association of HARS with the multiple ARS complex (pfam00458 in the NCBI Conserved Domain Database). Interestingly, glycyl-tRNA synthetase (GARS) has a similar *N*-terminal domain [Antonellis et al., 2003] and, to date, no disease-associated mutations have been identified therein. Arginine 137, glycine 205, valine 238, and lysine 376 reside within the catalytic core of the enzyme and proline 505 resides within the tRNA-binding domain (Fig. 1C). Thus, the variants that affect these amino acids may be detrimental to enzyme kinetics or tRNA recognition. Importantly, previously described disease-associated ARS mutations impair these two processes [Antonellis and Green, 2008; Antonellis et al., 2006; Latour et al., 2010; McLaughlin et al., 2010, 2012; Nangle et al., 2007].

p.Arg137Gln *HARS* Represents a Loss-of-Function Allele In Vivo

Yeast complementation assays have been successfully employed to evaluate the functional consequences of *GARS*, *YARS*, *AARS*, and *KARS* mutations. [Antonellis et al., 2006; Jordanova et al., 2006; McLaughlin et al., 2010, 2012]. Importantly, each ARS allele that is unable to complement deletion of the yeast ortholog is also unable to charge tRNA molecules as assessed by in vitro aminoacylation assays indicating that yeast is a relevant in vivo model to test for a loss-of-function effect [Antonellis et al., 2006; Jordanova et al., 2006; McLaughlin et al., 2010, 2012; Nangle et al., 2007]. To experimentally evaluate p.Arg137Gln, p.Gly205Asp, p.Val238Ala, p.Lys376Arg, and p.Pro505Ser *HARS* for a loss-of-function effect in vivo, we modeled the missense changes in the yeast ortholog *HTS1* (Table 3) and tested the ability of each variant to support yeast cell growth in complementation assays—p.Ala5Glu *HARS* was not modeled due to the inability to predict the orthologous residue in yeast (Fig. 1B). Briefly, a haploid yeast strain was generated with the endogenous *HTS1* gene deleted (*hts1*Δ) and viability supported via a maintenance vector consisting of a wild-type copy of *HTS1* on a *URA3*-bearing plasmid (pRS316). Experimental alleles were generated on a *LEU2*-bearing vector (pRS315), transformed into the above strain, and viability assessed by analysis of growth on 5-fluoroorotic acid (5-FOA), which selects for spontaneous loss of the *URA3*-bearing maintenance vector [Boeke et al., 1984]. The wild-type *HTS1* vector supported significant growth, while an insert-free pRS315 construct did not (Fig. 2A), consistent with our experimental vector

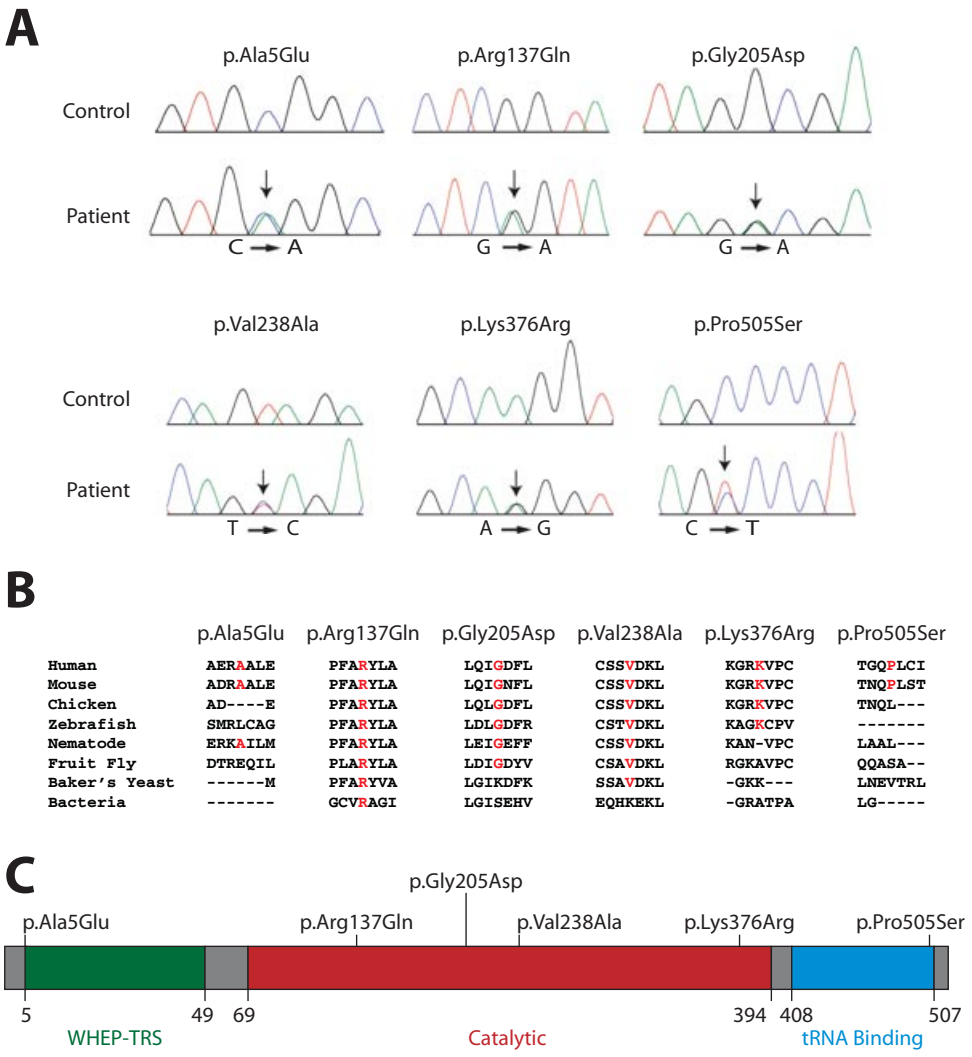

Figure 1. Identification, conservation, and localization of *HARS* variants. **A:** Representative sequence chromatograms are shown for the regions encompassing each identified *HARS* variant. Arrows indicate the position of each variant (present in the heterozygous state), with the nucleotide changes shown below and the predicted amino acid changes depicted above. **B:** Multiple-species protein alignments were generated to assess the conservation of affected amino acid residues. For each of the detected variants, the affected amino acid is shown along with the flanking HARS protein sequence in multiple, evolutionarily diverse species (indicated on the left). Note that the amino acid change is provided at the top, with conservation indicated in red for each protein sequence. **C:** HARS variants were mapped to the known functional domains of the protein, indicated in green (WHEP-TRS), red (catalytic domain), and blue (tRNA binding domain). The position of each domain along the protein is indicated below the cartoon.

harboring a functional copy of *HTS1*, and with *HTS1* being an essential gene, respectively. The p.Gly205Asp, p.Val238Ala, p.Lys376Arg, and p.Pro505Ser *HTS1* variants allowed growth in a manner consistent with wild-type *HTS1*. Because p.Val238Ala and p.Pro505Ser *HARS* were not detected in the public variant databases (Table 1), we further explored them for a loss of function via growth curve analysis. Neither of these variants grew in a manner significantly different from wild-type *HTS1* over a 25-hr period (Fig. 2B). In contrast to the above results, p.Arg137Gln *HTS1* could not complement the *hts1*Δ allele (Fig. 2A). Combined, our functional and computational analyses strongly suggest that p.Arg137Gln represents a loss-of-function allele and that it is the most likely of the *HARS* variants to be pathogenic. This notion is based on observations that previously identified disease-associated ARS mutations occur at highly conserved amino acids, are computationally predicted to be pathogenic, and cause a loss of function in aminoacylation and yeast growth assays [Antonellis et al., 2003, 2006; Jordanova et al., 2006; Latour et al., 2010; McLaughlin et al., 2010, 2012; Nangle et al., 2007].

Clinical Evaluation of Patients Carrying the p.Arg137Gln *HARS* Allele

The p.Arg137Gln *HARS* variant was identified in a patient with sporadic motor and sensory peripheral neuropathy, with sensory deficits more severe than motor deficits. At examination, the patient was a 64-year-old male with a 15-year history of impaired sensation in the lower extremities. There was no history of painless ulcers and he suffered from shooting pains in his legs over the

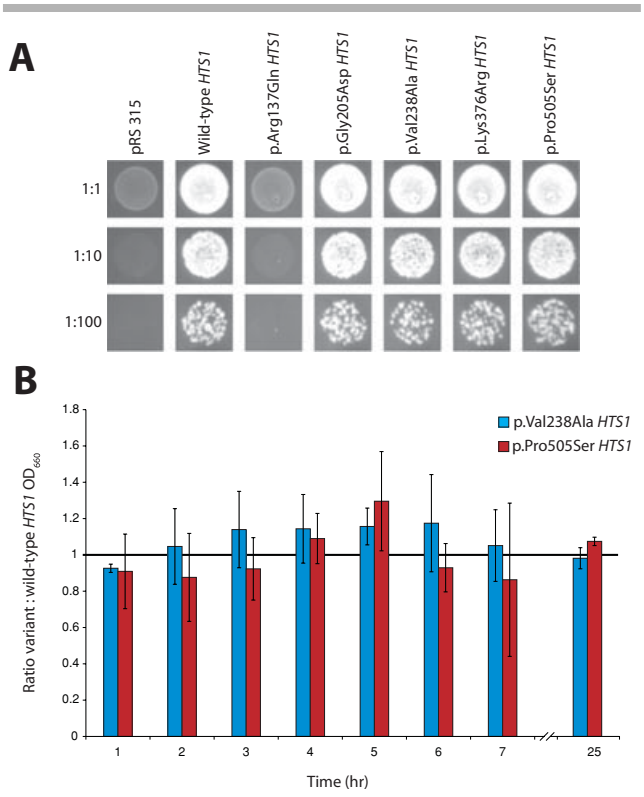

Figure 2. Growth of yeast strains expressing wild-type and mutant *HTS1*. **A:** Representative cultures of each yeast strain (indicated along the top of the panel) were inoculated and grown on solid growth medium containing 5-FOA at the indicated culture dilutions (1:1, 1:10, or 1:100). Each strain was previously transfected with a vector containing no insert ("pRS315"), wild-type *HTS1,* or the indicated mutant form of *HTS1* that modeled a human *HARS* mutation (see text). Identical results were obtained using two *hts1*Δ haploid yeast strains and three independently generated sets of *HTS1* expression constructs (data not shown). **B:** Growth curve analysis of *HTS1* variants. Yeast cultures were grown in SD media lacking leucine over 25 hr and the OD_{660} was monitored. The mean values obtained from three replicates of yeast cell growth associated with variant *HTS1* are expressed as a ratio to the growth of three replicates of wild-type *HTS1*. Error bars indicate standard deviation.

previous 4 years. Pes cavus and hammer toes were absent and there was no overt muscle wasting. There were brisk knee jerks, absent ankle jerks, and the plantar reflexes were flexor. Previous nerve conduction studies at age 57 showed a mild slowing of peroneal motor conduction velocity at 37 m/sec with a distal latency of 6.6 m/sec and an amplitude of 5.60 microvolts, and a sural sensory amplitude of 6.5 uV. At age 64, there were absent sural responses and a borderline reduced (10 uV) and delayed (3.82 m/sec) median sensory action potential. The peroneal motor action potential was not obtained and the median motor conduction velocity was 50 m/sec. Combined, these data indicate a neuropathy of axonal (or mixed axonal and demyelinating) origin. Interestingly, neurological examination of the 57 year-old female ClinSeq™ subject who is a carrier of p.Arg137Gln *HARS* (Table 1) did not reveal peripheral neuropathy—Sanger sequencing confirmed that this individual indeed carries this variant (data not shown). Given the late age of disease onset in the original patient and the incomplete penetrance of certain neuropathy-associated ARS mutations [Dubourg et al., 2006; Sivakumar et al., 2005], determining the pathogenic potential of p.Arg137Gln *HARS* in a relevant animal model system was considered essential for confirming the pathogenicity.

p.Arg137Gln *HARS* is Toxic to Neurons In Vivo

To evaluate the neurotoxicity of p.Arg137Gln *HARS*, we used the genetically tractable soil nematode, *C. elegans,* as an experimental model. As in humans, the *C. elegans* genome contains a single gene encoding cytoplasmic *HARS* (*hars-1*). The *C. elegans* HARS-1 protein is 54% identical and 70% similar to the human ortholog HARS (data not shown). Due to the conservation of arginine 137 between human and worm (Fig. 1B), we hypothesized that *C. elegans hars-1* might be used as a template to screen and differentiate mutations that impart neuronal toxicity in vivo. To this end, we overexpressed *C. elegans hars-1* variants specifically in GABAergic neurons, most of which are subclasses of motor neurons in nematode, to determine if p.Arg137Gln is sufficient to cause functional motor neuron defects. To engineer the GABA motor neuron specific expression of HARS-1 in *C. elegans*, a chimeric transgene was constructed in which the promoter region of the *C. elegans unc-25* gene, which encodes for glutamic acid decarboxylase, directs the expression of a full-length wild-type or p.Arg137Gln *hars-1* cDNA (P*unc-25*::*hars-1* [WT] or P*unc-25*::*hars-1* [p.Arg137Gln]) [Schuske et al., 2004]. To assay motor neuron abnormalities associated with transgene expression, the P*unc-25*::*hars-1* (WT or p.Arg137Gln) transgene was introduced into an integrated strain containing the *oxIs12* reporter transgene [McIntire et al., 1997], which expresses GFP under the control of the GABA motor neuron specific *unc-47* promoter [P*unc-47*::GFP] (Fig. 3A and B). This strain allows for the visualization of all GABA motor neuron cell bodies and their fine axonal processes (Fig. 3B). Motor neuron specific expression of p.Arg137Gln, but not WT, induced significant morphological abnormalities in GABA motor neurons (Fig. 3C and D). Expression of the p.Arg137Gln variant resulted in aberrant commissural axonal processes in ~40% of animals analyzed at three different developmental stages (L4, 1-day adult, and 4-day adult; Fig. 3G). Specifically, animals bearing the p.Arg137Gln transgene exhibited gross morphological defects in commissural axons, denoted by failure to reach the dorsal nerve cord, axonal beading, defasiculation, and breaks in the visualized GABAergic dorsal nerve cord (Fig. 3D). None of these defects were observed in transgenic control animals or animals over-expressing a wild-type transgene (Fig. 3B and C).

To determine if the morphological aberrations observed in the p.Arg137Gln transgenic animals were due to mislocalization of the HARS-1 protein, we constructed wild-type and p.Arg137Gln GFP fusion proteins directed by the *unc-25* promoter (P*unc-25*::GFP-*hars-1* [WT] or P*unc-25*::GFP-*hars-1* [p.Arg137Gln]). Heritable transgenic strains were generated by microinjection into N2 wild-type *C. elegans* strains [Mello and Fire, 1995; Mello et al., 1991]. Both the wild-type and p.Arg137Gln GFP fusion proteins localized specifically to GABA motor neurons and GFP was observed in the cell bodies and axonal processes (Fig. 3E and F). Importantly, the GFP-p.Arg137Gln fusion protein was able to recapitulate many of the axonal defects observed in transgenic animals overexpressing the nontagged p.Arg137Gln variant (Fig. 3F)—these defects were not seen in animals expressing the wild-type HARS-1 GFP fusion protein (Fig. 3E).

Lastly, we tested whether GABA neuron-specific expression of *hars-1* transgenes could induce motor performance defects. In addition to aberrant commissural axonal processes, p.Arg137Gln transgenic animals displayed mild locomotor defects on agar plates, whereas wild-type expressing strains appeared normal (data not

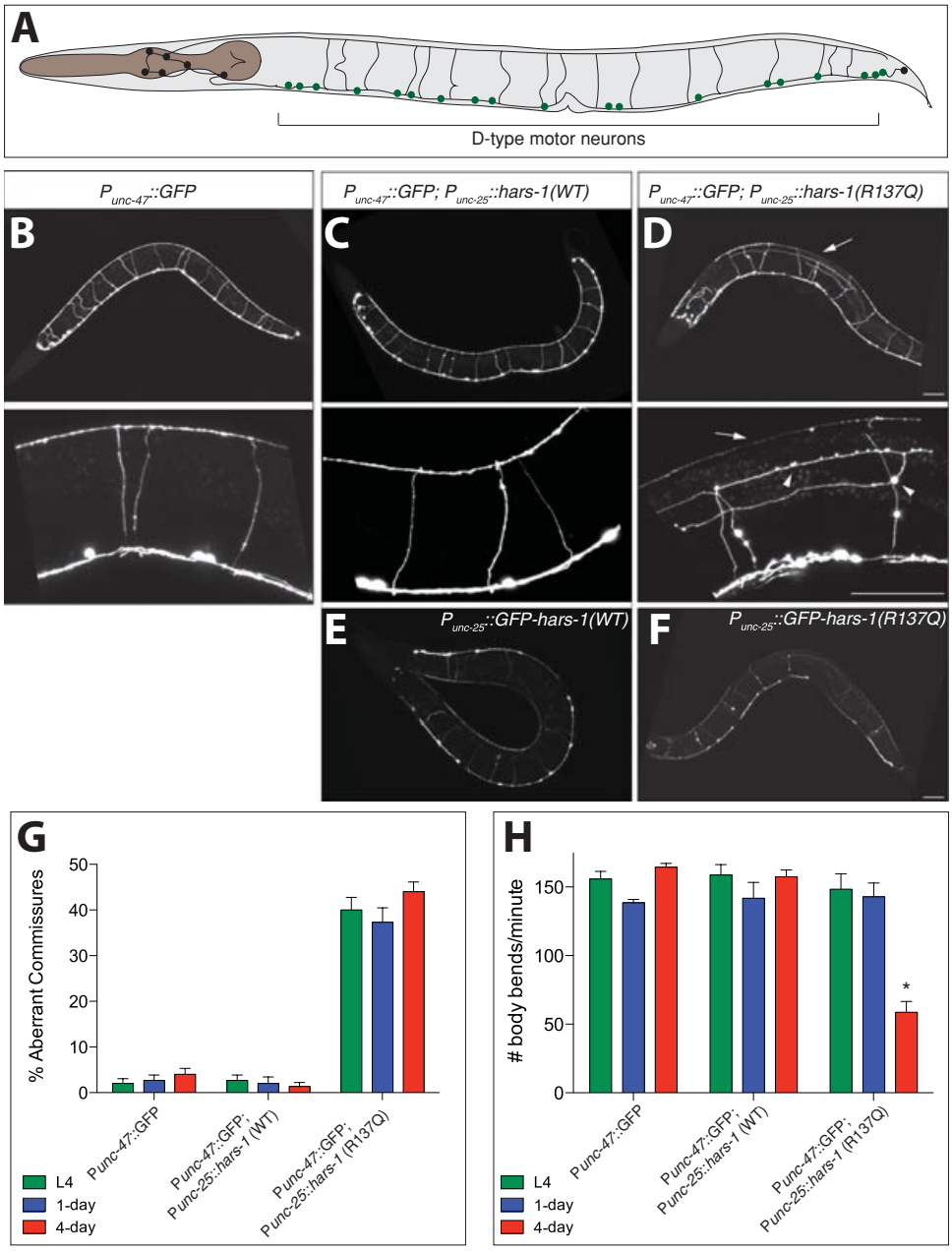

Figure 3. Neurotoxic effect of p.Arg137Gln (R137Q) *hars-1* expression in *C. elegans* motor neurons. **A:** Schematic diagram of the DD and VD motor neuron cell bodies (green dots) and commissural axons. (**B**–**D**) Confocal images of representative animals: anterior is to the left and dorsal is up. All animals in **B**–**D** are in the *oxIs12*[P*unc-47*::GFP]X background to visualize the DD and VD motor neuron axonal processes (scale bar: 50 μm). **B:** Control P*unc-47*::GFP animals display stereotyped commissural processes which all reach the dorsal cord. **C:** Animals expressing wild-type HARS-1 specifically in GABA motor neurons (P*unc-25*::*hars-1* [WT]) display normal commissural processes that reach the dorsal cord. **D:** Specific expression of mutant HARS-1 (R137Q) in GABA motor neurons results in abnormal commissural axonal phenotypes, denoted by prominent axonal beading (arrowheads) and thinning of the dorsal nerve cord (arrow). **E:** Expression of a wild-type GFP-HARS-1 (WT) fusion protein in GABA motor neurons displays protein localization throughout the cell body and axonal processes in wild-type animals. **F:** Mutant GFP-HARS-1 (R137Q) fusion protein expressed in GABA motor neurons displays a similar expression pattern as the wild-type fusion protein, but results in abnormal commissural axonal phenotypes when expressed in wild-type animals. **G:** Quantification of abnormal GABA motor neuron axonal commissures in mutant HARS-1 (R137Q) expressing animals (n = 50 worms/genotype; N = 3 trials/genotype, error bars ± S.E.M). **H:** Thrash assay quantifying movement defects. Mutant HARS-1(R137Q) expressing animals exhibit a progressive loss of motor coordination. (error bars ± S.E.M., $*P < 0.005$, n = 10/genotype).

shown). These defects were more severe in liquid media where thrashing rates [Miller et al., 1996] of p.Arg137Gln transgenics were significantly lower than the control or wild-type expressing strains (Fig. 3H). Interestingly, the aberrant axonal phenotype was present at L4 through 4-day adults, but the functional defect only manifests in 4-day adults (Fig. 3H). These data suggest that the p.Arg137Gln mutant exhibits a progressive loss of motor neuron function and coordination. Taken together, the in vivo morphological and functional defects suggest that p.Arg137Gln *HARS* imparts a cell autonomous neurotoxicity to motor neurons.

Discussion

Here, we describe mutation analysis of the *HARS* gene in patients with peripheral neuropathy. Six missense variants were identified and characterized, and computational and functional analyses revealed the following features of the p.Arg137Gln *HARS* variant: (1) location within the catalytic domain of the HARS protein and at an amino-acid residue conserved between human and bacteria; (2) loss-of-function based on yeast complementation assays; and (3) dominant toxicity to neurons in a *C. elegans* model. Importantly, we have recently validated the *C. elegans* model of neurotoxicity via analysis of the most common neuropathy-associated ARS mutation, R329H alanyl-tRNA synthetase ([*AARS*]; A.A. Beg, personal communication, 2011). Combined, these data indicate that p.Arg137Gln *HARS* may be a pathogenic allele similar to other disease-associated ARS mutations—such mutations are found in patients with motor and sensory peripheral neuropathy and an axonal pathology, cause a loss of function in tRNA charging, yeast viability, or proper localization within axons, and are dominantly toxic to axons in animal model systems [Antonellis et al., 2003, 2006; Jordanova et al., 2006; Latour et al., 2010; McLaughlin et al., 2010, 2012; Nangle et al., 2007; Seburn et al., 2006; Storkebaum et al., 2009]. Furthermore, arginine 137 resides in the BM12 domain of the HARS protein, which is involved in enzyme dimerization [Freist et al., 1999]—the majority of disease-associated *GARS* mutations also affect amino acids that reside on the dimer interface [Cader et al., 2007; He et al., 2011; Nangle et al., 2007; Xie et al., 2007]. Our findings expand the panel of loss-of-function human ARS alleles, and the data from our worm experiments indicate that p.Arg137Gln *HARS* is toxic to neurons in vivo.

The mechanistic link between heterozygosity for loss-of-function ARS alleles and axonal degeneration remains unknown. Haploinsufficiency of tRNA charging seems an unlikely explanation based on data showing that most disease-associated mutations are missense changes and that heterozygosity for a *Gars* null allele does not cause neuropathy in mouse [Seburn et al., 2006]. One possibility is that mutant ARS monomers interfere with the activity of the wild-type protein by a dominant-negative effect. This is consistent with the observation that all ARS enzymes implicated in axonal degeneration to date act as oligomers—HARS functions as a homodimer [Freist et al., 1999] and p.Arg137Gln does not affect enzyme dimerization (data not shown). This possibility is further supported by the identification of compound heterozygosity for a null allele and a hypomorphic allele at the lysyl-tRNA synthetase (*KARS*) locus in a patient with peripheral neuropathy [McLaughlin et al., 2010]. The combination of these alleles is predicted to cause a depletion of KARS activity below 50% and to possibly cross a threshold of tRNA charging required for axon function. However, overexpression of wild-type human GARS in two mouse models of dominant peripheral neuropathy caused by heterozygosity for *Gars* mutations did not dramatically improve the phenotype [Motley et al., 2011], indicating that any dominant-negative effect may be irreversible. However, it will be important to determine if wild-type HARS-1 can complement the toxicity of p.Arg137Gln HARS-1 in a stable transgenic *C. elegans* model system using Mos1-mediated transgenesis. Another possibility is that impaired tRNA charging or impaired ARS localization are prerequisites for some undefined gain-of-function toxicity to axons (e.g., these RNA-binding proteins may now be free to inappropriately interact with RNA molecules in the axon or nerve cell body). Finally, the neurotoxic effect of ARS mutations is unlikely to involve mitochondrial enzyme function. Although GARS and KARS charge tRNA in both the cytoplasm and mitochondria, YARS, AARS, and HARS are predicted to charge tRNA only in the cytoplasm. Furthermore, disease-associated mutations in the genes encoding mitochondrial ARS enzymes (*AARS2*, *DARS2*, *EARS2*, *HARS2*, *MARS2*, *RARS2*, *SARS2*, and *YARS2*) are not associated with an overt axonal neuropathy [Bayat et al. 2012; Belostotsky et al. 2011; Edvardson et al., 2007; Gotz et al. 2011; Pierce et al. 2011; Riley et al. 2010; Scheper et al., 2007; Steenweg et al. 2012]; however, detailed neurological examinations of patients with mitochondrial ARS mutations will be required to rule out such a phenotype.

Inherited peripheral neuropathies are clinically and genetically heterogenous with variable age of onset and reduced penetrance associated with specific loci. Moreover, the extent to which genetic (i.e., due to inherited or de novo mutations) versus environmental causes (e.g., diabetes and vitamin deficiencies) account for the 10% prevalence of peripheral neuropathy in the aging population [Martyn and Hughes, 1997] is unknown. As such, these diseases present a major challenge for the identification and validation of disease-causing or disease-modifying variants, especially when faced with small pedigrees or sporadic cases with one or both biological parents unavailable to evaluate for de novo mutations, thus hindering the ability to build a robust genetic argument. Indeed, the identification of p.Arg137Gln *HARS* in one affected and one unaffected individual underscores the importance of informative functional analyses. The studies outlined here have two major implications for the above challenges. First, we present a pipeline to rapidly assess ARS alleles for impaired function and axonal toxicity in vivo. This approach will aid in the distinction between pathogenic and non-pathogenic ARS alleles and is feasible for variants identified at all 37 human ARS loci [Antonellis and Green, 2008]. Second, these findings underscore the importance of identifying ARS alleles with neurotoxic potential in patient cohorts or in the general population. Alleles such as p.Arg137Gln *HARS* may directly predispose patients to peripheral neuropathy or may modify a peripheral neuropathy phenotype by contributing to the genetic and environmental load [Lupski et al., 2011] in a given patient. However, although our functional analyses revealed a loss-of-function neurotoxic *HARS* allele, the causal link between *HARS* mutations and peripheral neuropathy remains unclear, largely due to the lack of a strong genetic argument. Studies designed to further screen relevant patient populations for *HARS* mutations, clinically evaluate other carriers of p.Arg137Gln *HARS*, and develop a mammalian model of p.Arg137Gln *HARS* will be critical for addressing this issue. In summary, our approaches and findings have important implications for understanding ARS variants and how they relate to human disease as well as a basis for understanding such variation in the context of gene–gene and gene–environment interactions.

Acknowledgments

We are indebted to the patients and their families for participating in this study. We thank Ellen Pederson, Bob Lyons, and the University of Michigan DNA Sequencing Core for sequencing and genotyping analysis; Jennifer Johnston for mutation validation; Marina Kennerson for additional patient information; Chani Hodonsky for expert technical assistance; Tom Wilson for instruction on yeast viability assays; Eric Green for ARS locus sequencing; Sundeep Kalantry for critical analysis of the manuscript; and Miriam Meisler and her laboratory for thoughtful discussions on the experiments and manuscript. Some nematode strains were provided by the *Caenorhabditis* Genetics Center.

References

Antonellis A, Ellsworth RE, Sambuughin N, Puls I, Abel A, Lee-Lin SQ, Jordanova A, Kremensky I, Christodoulou K, Middleton LT, Sivakumar K, Ionasescu V,

et al., 2003. Glycyl tRNA synthetase mutations in Charcot–Marie–Tooth disease type 2D and distal spinal muscular atrophy type V. Am J Hum Genet 72:1293–1299.

Antonellis A, Green ED. 2008. The role of aminoacyl-tRNA synthetases in genetic diseases. Annu Rev Genomics Hum Genet 9:87–107.

Antonellis A, Lee-Lin SQ, Wasterlain A, Leo P, Quezado M, Goldfarb LG, Myung K, Burgess S, Fischbeck KH, Green ED. 2006. Functional analyses of glycyl-tRNA synthetase mutations suggest a key role for tRNA-charging enzymes in peripheral axons. J Neurosci 26:10397–10406.

Bayat V, Thiffault I, Jaiswal M, Tetreault M, Donti T, Sasarman F, Bernard G, Demers-Lamarche J, Dicaire MJ, Mathieu J, Vanasse M, Bouchard JP, et al., 2012. Mutations in the mitochondrial methionyl-tRNA synthetase cause a neurodegenerative phenotype in flies and a recessive ataxia (ARSAL) in humans. PLoS Biol 10:e1001288.

Belostotsky R, Ben-Shalom E, Rinat C, Becker-Cohen R, Feinstein S, Zeligson S, Segel R, Elpeleg O, Nassar S, Frishberg Y. 2011. Mutations in the mitochondrial seryl-tRNA synthetase cause hyperuricemia, pulmonary hypertension, renal failure in infancy and alkalosis, HUPRA syndrome. Am J Hum Genet 88:193–200.

Biesecker LG, Mullikin JC, Facio FM, Turner C, Cherukuri PF, Blakesley RW, Bouffard GG, Chines PS, Cruz P, Hansen NF, Teer JK, Maskeri B, et al., 2009. The ClinSeq Project: piloting large-scale genome sequencing for research in genomic medicine. Genome Res 19:1665–1674.

Boeke JD, LaCroute F, Fink GR. 1984. A positive selection for mutants lacking orotidine-5′-phosphate decarboxylase activity in yeast: 5-fluoro-orotic acid resistance. Mol Gen Genet 197:345–346.

Brenner S. 1974. The genetics of *Caenorhabditis elegans*. Genetics 77:71–94.

Cader MZ, Ren J, James PA, Bird LE, Talbot K, Stammers DK. 2007. Crystal structure of human wildtype and S581L-mutant glycyl-tRNA synthetase, an enzyme underlying distal spinal muscular atrophy. FEBS Lett 581:2959–2964.

Cheng J, Randall A, Baldi P. 2006. Prediction of protein stability changes for single-site mutations using support vector machines. Proteins 62:1125–1132.

Dubourg O, Azzedine H, Yaou RB, Pouget J, Barois A, Meininger V, Bouteiller D, Ruberg M, Brice A, LeGuern E. 2006. The G526R glycyl-tRNA synthetase gene mutation in distal hereditary motor neuropathy type V. Neurology 66:1721–1726.

Dyck PJ, Lambert EH. 1968. Lower motor and primary sensory neuron diseases with peroneal muscular atrophy. II. Neurologic, genetic, and electrophysiologic findings in various neuronal degenerations. Arch Neurol 18:619–625.

Edvardson S, Shaag A, Kolesnikova O, Gomori JM, Tarassov I, Einbinder T, Saada A, Elpeleg O. 2007. Deleterious mutation in the mitochondrial arginyl-transfer RNA synthetase gene is associated with pontocerebellar hypoplasia. Am J Hum Genet 81:857–862.

Freist W, Verhey JF, Ruhlmann A, Gauss DH, Arnez JG. 1999. Histidyl-tRNA synthetase. Biol Chem 380:623–646.

Gotz A, Tyynismaa H, Euro L, Ellonen P, Hyotylainen T, Ojala T, Hamalainen RH, Tommiska J, Raivio T, Oresic M, Karikoski R, Tammela O, et al., 2011. Exome sequencing identifies mitochondrial alanyl-tRNA synthetase mutations in infantile mitochondrial cardiomyopathy. Am J Hum Genet 88:635–642.

Green ED, Birren B, Klapholz S, Myers RM, Riethman H, Roskams J. 1999. Genome analysis: a laboratory manual. Cold Spring Harbor, NY: Cold Spring Harbor Laboratory Press.

He W, Zhang HM, Chong YE, Guo M, Marshall AG, Yang XL. 2011. Dispersed disease-causing neomorphic mutations on a single protein promote the same localized conformational opening. Proc Natl Acad Sci USA 108:12307–12312.

Hobert O. 2002. PCR fusion-based approach to create reporter gene constructs for expression analysis in transgenic *C. elegans*. Biotechniques 32:728–730.

Jordanova A, Irobi J, Thomas FP, Van Dijck P, Meerschaert K, Dewil M, Dierick I, Jacobs A, De Vriendt E, Guergueltcheva V, Rao CV, Tournev I, et al., 2006. Disrupted function and axonal distribution of mutant tyrosyl-tRNA synthetase in dominant intermediate Charcot–Marie–Tooth neuropathy. Nat Genet 38:197–202.

Larkin MA, Blackshields G, Brown NP, Chenna R, McGettigan PA, McWilliam H, Valentin F, Wallace IM, Wilm A, Lopez R, Thompson JD, Gibson TJ, et al., 2007. Clustal W and Clustal X version 2.0. Bioinformatics 23:2947–2948.

Latour P, Thauvin-Robinet C, Baudelet-Mery C, Soichot P, Cusin V, Faivre L, Locatelli MC, Mayencon M, Sarcey A, Broussolle E, Camu W, David A, et al., 2010. A major determinant for binding and aminoacylation of tRNA (Ala) in cytoplasmic Alanyl-tRNA synthetase is mutated in dominant axonal Charcot–Marie–Tooth disease. Am J Hum Genet 86:77–82.

Lupski JR, Belmont JW, Boerwinkle E, Gibbs RA. 2011. Clan genomics and the complex architecture of human disease. Cell 147:32–43.

Martyn CN, Hughes RA. 1997. Epidemiology of peripheral neuropathy. J Neurol Neurosurg Psychiatr 62:310–318.

McIntire SL, Reimer RJ, Schuske K, Edwards RH, Jorgensen EM. 1997. Identification and characterization of the vesicular GABA transporter. Nature 389:870–876.

McLaughlin HM, Sakaguchi R, Giblin W, Wilson TE, Biesecker L, Lupski JR, Talbot K, Vance JM, Zuchner S, Lee YC, Kennerson M, Hou YM, et al., 2012. A recurrent loss-of-function alanyl-tRNA synthetase (AARS) mutation in patients with Charcot–Marie–Tooth disease type 2N (CMT2N). Hum Mutat 33:244–253.

McLaughlin HM, Sakaguchi R, Liu C, Igarashi T, Pehlivan D, Chu K, Iyer R, Cruz P, Cherukuri PF, Hansen NF, Mullikin JC, NISC Comparative Sequencing Program, et al., 2010. Compound heterozygosity for loss-of-function lysyl-tRNA synthetase mutations in a patient with peripheral neuropathy. Am J Hum Genet 87:560–566.

Mello C, Fire A. 1995. DNA transformation. Methods Cell Biol 48:451–482.

Mello CC, Kramer JM, Stinchcomb D, Ambros V. 1991. Efficient gene transfer in *C.elegans*: extrachromosomal maintenance and integration of transforming sequences. EMBO J 10:3959–3970.

Miller KG, Alfonso A, Nguyen M, Crowell JA, Johnson CD, Rand JB. 1996. A genetic selection for *Caenorhabditis elegans* synaptic transmission mutants. Proc Natl Acad Sci USA 93:12593–12598.

Motley WW, Seburn KL, Nawaz MH, Miers KE, Cheng J, Antonellis A, Green ED, Talbot K, Yang XL, Fischbeck KH, Burgess RW. 2011. Charcot–Marie–Tooth-linked mutant GARS is toxic to peripheral neurons independent of wild-type GARS levels. PLoS Genet 7:e1002399.

Nangle LA, Zhang W, Xie W, Yang XL, Schimmel P. 2007. Charcot–Marie–Tooth disease-associated mutant tRNA synthetases linked to altered dimer interface and neurite distribution defect. Proc Natl Acad Sci USA 104:11239–11244.

Pierce SB, Chisholm KM, Lynch ED, Lee MK, Walsh T, Opitz JM, Li W, Klevit RE, King MC. 2011. Mutations in mitochondrial histidyl tRNA synthetase HARS2 cause ovarian dysgenesis and sensorineural hearing loss of Perrault syndrome. Proc Natl Acad Sci USA 108:6543–6548.

Riley LG, Cooper S, Hickey P, Rudinger-Thirion J, McKenzie M, Compton A, Lim SC, Thorburn D, Ryan MT, Giege R, Bahlo M, Christodoulou J. 2010. Mutation of the mitochondrial tyrosyl-tRNA synthetase gene, YARS2, causes myopathy, lactic acidosis, and sideroblastic anemia—MLASA syndrome. Am J Hum Genet 87:52–59.

Scheper GC, van der Klok T, van Andel RJ, van Berkel CG, Sissler M, Smet J, Muravina TI, Serkov SV, Uziel G, Bugiani M, Schiffmann R, Krageloh-Mann I, et al., 2007. Mitochondrial aspartyl-tRNA synthetase deficiency causes leukoencephalopathy with brain stem and spinal cord involvement and lactate elevation. Nat Genet 39:534–539.

Schuske K, Beg AA, Jorgensen EM. 2004. The GABA nervous system in *C. elegans*. Trends Neurosci 27:407–414.

Seburn KL, Nangle LA, Cox GA, Schimmel P, Burgess RW. 2006. An active dominant mutation of glycyl-tRNA synthetase causes neuropathy in a Charcot–Marie–Tooth 2D mouse model. Neuron 51:715–726.

Sivakumar K, Kyriakides T, Puls I, Nicholson GA, Funalot B, Antonellis A, Sambuughin N, Christodoulou K, Beggs JL, Zamba-Papanicolaou E, Ionasescu V, Dalakas MC, et al., 2005. Phenotypic spectrum of disorders associated with glycyl-tRNA synthetase mutations. Brain 128:2304–2314.

Steenweg ME, Ghezzi D, Haack T, Abbink TE, Martinelli D, van Berkel CG, Bley A, Diogo L, Grillo E, Te Water Naude J, Strom TM, Bertini E, et al., 2012. Leukoencephalopathy with thalamus and brainstem involvement and high lactate 'LTBL' caused by EARS2 mutations. Brain 135:1387–1394.

Storkebaum E, Leitao-Goncalves R, Godenschwege T, Nangle L, Mejia M, Bosmans I, Ooms T, Jacobs A, Van Dijck P, Yang XL, Shimmel P, Norga K, et al., 2009. Dominant mutations in the tyrosyl-tRNA synthetase gene recapitulate in Drosophila features of human Charcot–Marie–Tooth neuropathy. Proc Natl Acad Sci USA 106:11782–11787.

Xie W, Nangle LA, Zhang W, Schimmel P, Yang XL. 2007. Long-range structural effects of a Charcot–Marie–Tooth disease-causing mutation in human glycyl-tRNA synthetase. Proc Natl Acad Sci USA 104:9976–9981.